

Journal Pre-proof

Synthesis and Thermal Decomposition of TNPG

Wen-qian Wu, Wei Feng, Qiu-han Lin, Shun-yao Wang, Zi-chao Guo, Li-ping Chen, Wang-hua Chen



PII: S0040-6031(19)30597-0
DOI: <https://doi.org/10.1016/j.tca.2019.178396>
Reference: TCA 178396

To appear in: *Thermochemica Acta*

Received Date: 27 June 2019
Revised Date: 31 August 2019
Accepted Date: 31 August 2019

Please cite this article as: Wu W-qian, Feng W, Lin Q-han, Wang S-yao, Guo Z-chao, Chen L-ping, Chen W-hua, Synthesis and Thermal Decomposition of TNPG, *Thermochemica Acta* (2019), doi: <https://doi.org/10.1016/j.tca.2019.178396>

This is a PDF file of an article that has undergone enhancements after acceptance, such as the addition of a cover page and metadata, and formatting for readability, but it is not yet the definitive version of record. This version will undergo additional copyediting, typesetting and review before it is published in its final form, but we are providing this version to give early visibility of the article. Please note that, during the production process, errors may be discovered which could affect the content, and all legal disclaimers that apply to the journal pertain.

© 2019 Published by Elsevier.

Synthesis and Thermal Decomposition of TNPG

Wen-qian Wu^a · Wei Feng^b · Qiu-han Lin^a · Shun-yao Wang^a · Zi-chao

Guo^{a,*} · Li-ping Chen^a · Wang-hua Chen^a

^a Department of Safety Engineering School of Chemical Engineering, Nanjing University of Science and Technology, Nanjing Jiangsu 210094, China

^b Xi'an Modern Chemistry Research Institute, Xi'an 710065, China

✉ gzc319@njust.edu.cn (Z.C. Guo).

Highlights

- TNPG was synthesized and its decomposition process has been thoroughly studied in this work.
- Thermal experiments prove that the decomposition of TNPG follows an autocatalytic behavior
- Kinetic model for TNPG decomposition process was established on the basis of DSC and ARC results.
- This work helps to establish dynamic models for the materials that present coupling endothermic with exothermic.

【ABSTRACT】 1, 3, 5-Trihydroxy-2, 4, 6-trinitrobenzene (TNPG) is an essential energetic intermediate for synthesis of 1, 3, 5-Triamino-2, 4, 6-Trinitrobenzene (TATB). The thermal stability of TNPG was studied in this work. First, TNPG was synthesized by nitration of 1, 3, 5-trihydroxybenzene with the solution feeding. Then, the thermal stability of TNPG was studied by DSC and ARC experiments. The non-isothermal DSC results indicated that the thermal decomposition of TNPG overlapped with the endothermic melting process. The isothermal DSC and ARC results evidenced that the decomposition of TNPG followed the autocatalytic mechanism. Two different models were constructed to depict the decomposition process of TNPG. By comparison with the isothermal DSC results, it was found that the following model could better describe the decomposition process of TNPG: $A \rightarrow B_S$ (autocatalytic), $A \rightarrow A_{liq}$ (melting), $A_{liq} \rightarrow B$

(autocatalytic).

【Keywords】 Nitrification; thermal decomposition; coupling; autocatalysis; kinetics

1. Introduction

1, 3, 5-Trihydroxy-2, 4, 6-trinitrobenzene (TNPG), a light yellow powder, is a strongly acidic compound and highly soluble in water. It can form metal salts that have strong combustion or explosive properties, for example, lead trinitrophenylglucinate is an important primer ^[1, 2]. Because its molecular structure contains three hydroxyl groups and three nitro groups, it is also an important explosive.

TNPG, as an insensitive and high-energy explosive intermediate, can achieve non-chlorination production of TATB ^[3-7], reduce production costs and improve the safety of experiments and production. In recent years, researchers have also developed insensitive high-energy explosives with eutectics that is formed from TNPG with high-nitrogen substances or basic compounds ^[8, 9] in the field of high-energy eutectic.

A large number of research works have been contributed to optimize the synthesis conditions for TNPG, including reaction temperature, material ratio, concentration, etc. There are also some reports aimed to study the relationship between structure and performance of TNPG ^[10-14]. However, the decomposition features of TNPG have not been thoroughly studied, which is crucial for storage and transportation of TNPG. In this work, TNPG will be first synthesized by nitration of phloroglucin with $\text{NH}_4\text{NO}_3/\text{H}_2\text{SO}_4$ system. Formation of TNPG are confirmed by FTIR and NMR tests. Then thermal analysis technology, say DSC and ARC, combined with thermal analysis software will be employed to study the decomposition features of TNPG.

2. Experiment and equipment

2.1. Reagents

Phloroglucinol (purity \geq 99%) was purchased from Maclean Biochemical Technology Co. in Shanghai, Ltd. Concentrated sulfuric acid was purchased from Shanghai Pharmaceutical Reagent Company of China Pharmaceutical Group (concentration 98%), A.R. Ammonium nitrate (AN), L.P.

2.2. Synthesis process of TNPG by phloroglucin nitration

TNPG is synthesized by nitration of phloroglucinol with $\text{NH}_4\text{NO}_3/\text{H}_2\text{SO}_4$ system. The synthesis route is as follows (Fig.1). The detailed synthesis procedure can be found in the Supplementary Profile.

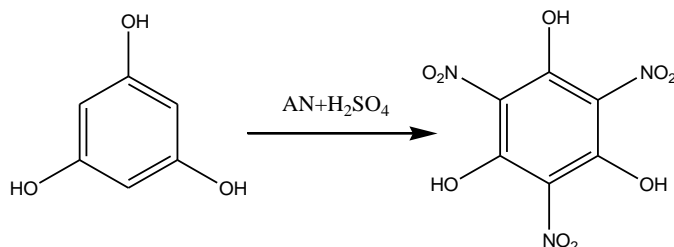


Fig. 1. The process of phloroglucin nitration

2.3. Equipment and characterization methods

2.3.1. Sample and equipment

Before the further study, the synthesized TNPG were tested by TG-DSC to determine the weight percent of crystal water. The result can be found in the Supplementary Profile (Fig. S3). About 2.25% weight percent of crystal water was confirmed in the synthesized TNPG. The mole ratio of TNPG to water is about 3:1. NICOLETIS10 Fourier infrared spectrometer, AVANCE III 500MHz NMR spectrometer are used to characterize the structure of TNPG. Differential scanning calorimeter DSC 1 from Swiss METTLER TOLEDO and the esARC adiabatic calorimeter from the THT Company are used to study its thermal decomposition.

2.3.2. Differential scanning calorimetry DSC

The test uses a closed high-pressure stainless steel crucible (HP steel) withstand pressure of 15 MPa. For the dynamic experiment, the sample is heated from 80-380 °C under the different temperature rise rates as 1, 2, 4, 8 K/min respectively. The atmosphere is nitrogen with a flow rate of 50 ml/min. In addition, the temperature for isothermal experiment are 145, 148, 150, 161, 163, 165 °C (that is, the furnace temperature can rise to the desired value at temperature rise rate of 200-300 K/min under program control, then put the sample into furnace and start the test).

2.3.3. Adiabatic calorimetry ARC

During the test, the prepared sample ball is heated to a preset initial temperature under adiabatic conditions. After a certain waiting time, the system achieves thermal balance. Once the sample begins to exothermic, the experimental system automatically

enters the strict adiabatic condition.

The sample cell used in this test was made by Hastelloy, and the test conditions are listed in Table 1. The thermal inertia factor φ is calculated by the following equation,

$$\varphi = 1 + \frac{M_{cell} c_{p,cell}}{M_{sample} c_{p,sample}} \quad (1)$$

Where M represents the mass, c_p is the heat capacity.

Table 1 The test conditions of ARC

m_s (g)	m_{ball} (g)	Temperature(°C)	Temperature step(°C)	Sensitivity(°C/min)	waiting time(min)
0.198	15.826	50-400	5	0.02	10

3. Results and discussion

3.1. Structural characterization of TNPG

The infrared spectrum of the product is tested as shown in Fig. S1. The H-NMR and C-NMR spectrum are shown in Fig. S2. These results confirmed the formation of TNPG. The yield of TNPG was calculated to be about 93%.

3.2. The DSC test results

3.2.1. Differential scanning calorimetry DSC

The dynamic DSC results are shown in Fig. 2 and summarized in Table 2. Obviously, TNPG is a material that has overlapping endothermic and exothermic processes during heating. The endothermic peaks at about 160 °C correspond to the melting process of TNPG^[12] and the exothermic peaks are the thermal decomposition process. It is obvious that the exothermic signal is sharp and narrow, indicating that the exothermic process may be autocatalytic^[15-18]. The average specific heat release at the four temperature rise rates is 3003 J/g. In fact, as shown in Fig. S3 in the Supplementary Profile, there is an endothermic process at about 100~120 °C, which corresponds to the loss process of the crystal water. This endothermic process is not illustrated in Fig. 2.

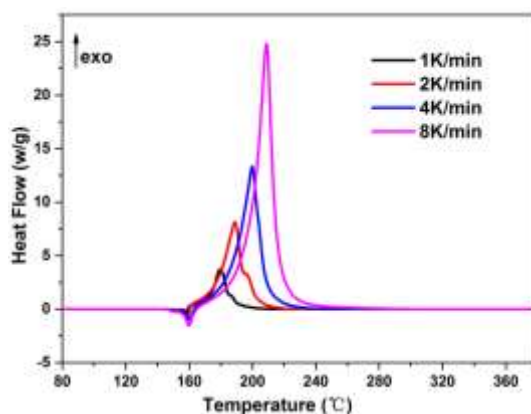


Fig. 2. Dynamic DSC curves of TNPG at 1, 2, 4, 8 K/min

Table 2 Thermal decomposition characteristic parameters of TNPG

β (K/min)	m (mg)	$T_{\text{endo}}(^{\circ}\text{C})^{\text{a}}$	$\Delta H_{\text{endo}}(\text{J/g})$	$T_{\text{onset}}(^{\circ}\text{C})$	$T_{\text{p}}(^{\circ}\text{C})$	$\Delta H_{\text{d}}(\text{J/g})$
1	0.82	158.6	135	174.9	180.0	-2403
2	0.83	159.1	152	177.3	188.8	-2912
4	0.84	160.5	123	187.1	199.8	-3224
8	0.82	162.5	96	200.1	211.2	-3473

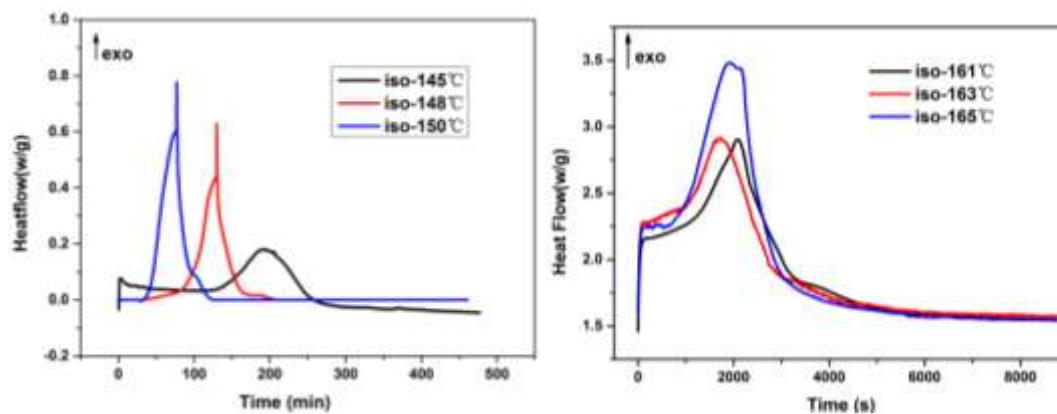
^a T_{endo} refer to the peak temperature of the endothermic process.

3.2.2. Isothermal experiment

The most straightforward way to verify the autocatalytic process is to conduct the isothermal experiments ^[16]. Different temperature below and above the melting point are selected for isothermal experiments respectively. The results are shown in Fig. 3. The heat flow profiles in Fig. 3(a) evidence that TNPG can decompose in the solid state because the isothermal temperatures in this figure are below the melting point. The heat flow profiles in Fig. 3(a) present “Bell” shape, indicating that the decomposition of TNPG in the solid state presents autocatalytic behavior ^[16-21]. The induction periods gradually reduce with the isothermal temperature increasing.

Since the isothermal temperature in Fig. 3(b) is higher than the melting point, the exothermic signals correspond to the decomposition process of TNPG in the liquid state. Obviously, since the heat flow profiles in Fig. 3(b) present the “Bell” shape, the decomposition process in the liquid state presents autocatalytic nature.

Moreover, from the dynamic DSC experiment, the decomposition process in liquid state is more intense and the decomposition rate is different from the solid state, so the heat release rate increases sharply and causes occurrence of “spikes”. At the same time, the consistence of two phases and purity of the substance resulting the unsmooth curves.



(a) The curve below the melting point

(b) The curve above the melting point

Fig. 3. The isothermal curves at different temperature

3.3. Adiabatic calorimetry test-ARC

To further investigate the thermal decomposition behaviors of TNPG, adiabatic calorimetry tests by ARC were conducted. The temperature and pressure profiles are shown in Fig.4 and the thermal decomposition parameters obtained are summarized in Table 3. From Fig. 4(a), the sample begins to decompose at about 150 °C, and as the temperature increases, the pressure during the decomposition gradually increases like Fig. 4(b). After about 30 minutes, the temperature and pressure rise sharply. The temperature drastically increased from 156 °C to 184 °C in three minutes and the corresponding pressure increased from 4.5 bar to 25 bar. This violent temperature increase is consistent with the sharp heat flow profiles of DSC tests.

In addition, the onset exothermic temperature (T_0) is 150 °C. This temperature is obviously lower than the melting point of TNPG, indicating that the decomposition process of TNPG could occur in the solid state. This result is in agreement with the isothermal DSC results in Fig. 3(a).

From Table 3, one can see that the value of the thermal inertia factor φ is as high as 17.78. The kinetics determined in this condition is unreliable. Therefore, the kinetic model and kinetic parameters will be calculated using the DSC results.

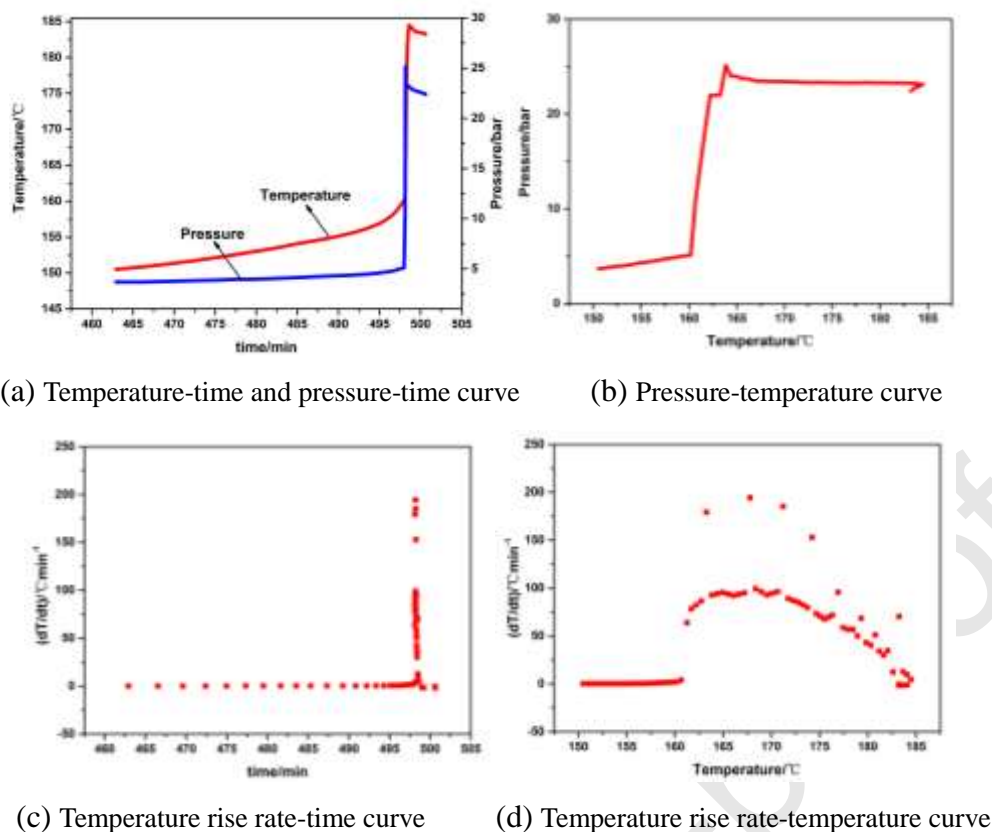


Fig. 4. The ARC test results for TNPG

Table 3 The thermal decomposition characteristic parameters of TNPG

$T_0(^{\circ}\text{C})$	$(dT/dt)_0$	$T_{max}(^{\circ}\text{C})$	$(dT/dt)_{max}$	$(dP/dt)_{max}$	$P_{max}(\text{bar})$	φ	$\Delta T_{ad}(^{\circ}\text{C})$
150.5	0.13	184.5	194.32	592.77	25.14	17.78	33.9

3.4. Kinetic analysis

3.4.1. Calculation of E and A

Before constructing the kinetic model, the initial value of activation energy (E) was calculated by Friedman^[16] and Kissinger methods^[17] respectively. The Friedman method was first used to observe the relationship between the activation energy E and the conversion α and judge whether the decomposition in the liquid state can be described by a single reaction. Then the value of activation energy was calculated by Kissinger method.

Using the Friedman method, reliable activation energy can be obtained without involving the mechanistic function. Equation (2) is the Friedman equation, from which the value of activation energy E at each reaction conversion α can be obtained^[22-26].

$$\ln [\beta (d\alpha/dT)]_{\alpha} = \ln [f(\alpha) A] - E/RT \quad (2)$$

Where β is the temperature rise rate, K/min; α is conversion; A is the pre-

exponential factor under the reaction conversion α , s^{-1} ; $f(\alpha)$ is the mechanism function; E is the activation energy, kJ/mol ; R is the ideal gas constant, $8.314 \text{ J/mol}\cdot\text{K}$; T is temperature, K .

The relationship between the E and α calculated by the Friedman method is shown in Fig. 5. We can see that within the conversion range from 0.1 to 0.9, there is no obvious fluctuations and the value of average E is about 97-103 kJ/mol , indicating that the thermal decomposition process in the liquid state can be described by one single reaction.

The Kissinger method considers that the reaction rate is the highest at the peak temperature T_{max} of the heat flow curve, and the non-isothermal and heterogeneous kinetic equation can be rewritten to the equation (3):

$$\ln(\beta/T_{max}^2) = \ln(RA/E) - E/RT_{max} \quad (3)$$

Where β is the temperature rise rate, K/min ; α is conversion; A is the pre-exponential factor, s^{-1} ; E is the activation energy, kJ/mol ; R is the ideal gas constant, $8.314 \text{ J/mol}\cdot\text{K}$.

T_{max} is obtained by a set of curves of TNPG at four temperature rise rates in Fig.2, and then a curve of $\ln(\beta/T_{max}^2)$ vs $1/T_{max}$ is obtained. The activation energy E and pre-exponential factor A is calculated from the slope and intercept from the fitted curve [23-27]. The experimental data was fitted using the Kissinger method and the results are shown in Fig. 6. The activation energy of the reaction is 113 kJ/mol , and the corresponding pre-exponential factor $\lg A$ is 8.8683 s^{-1} . The result shows the activation energy of TNPG decomposition calculated by the Friedman method and the Kissinger method are similar.

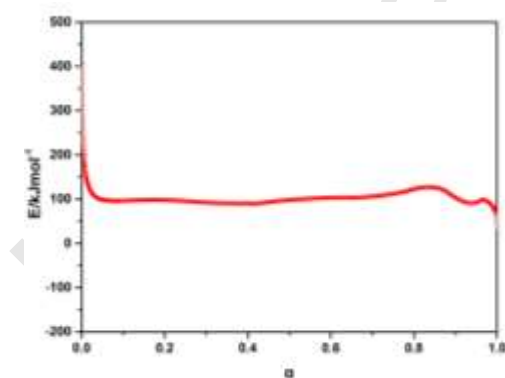


Fig.5. Relationship of E and α

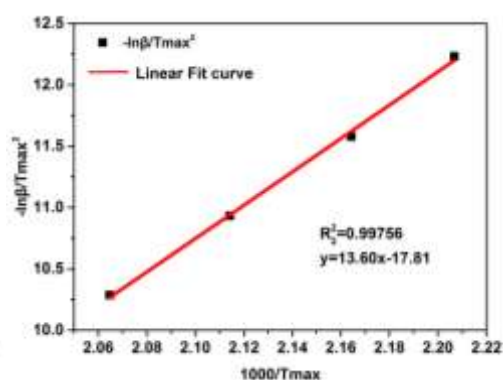


Fig.6. Fitting results of Kissinger method

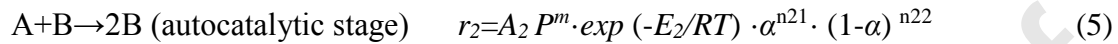
3.4.2. Construction of reaction model

In this section, two reaction models will be constructed to depict the thermal behaviors of TNPG decomposition. The Thermal Safety Software (TSS) developed by

St. Petersburg Chemical Information Company [27-29] is used to establish the reaction model and fit the kinetic parameters.

Model 1- construction reaction model with exothermal data

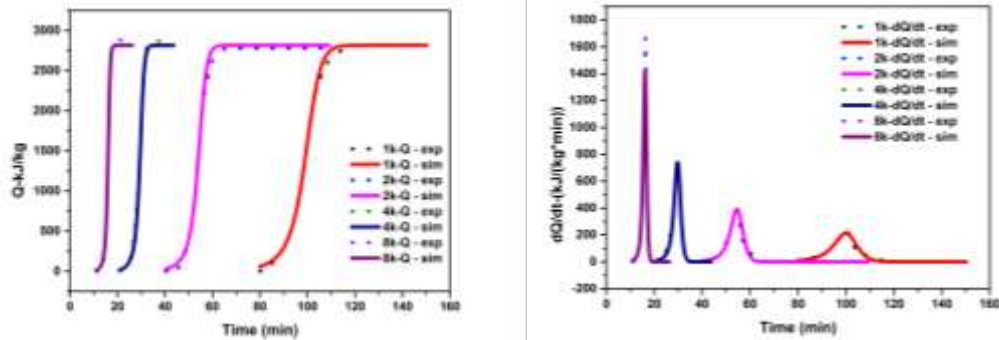
Based on the previous results, the decomposition of TNPG in liquid state can be depicted by one single reaction that presents strongly autocatalytic behavior. The traditional SB model ignores the initial stage of the autocatalytic reaction. Herein, the autocatalytic model including the initial reaction was employed as follows:



Then its kinetic expression can be described as:

$$d\alpha/dt = r_1 + r_2 = A_0 P^m \cdot \exp(-E/RT) \cdot (1-\alpha)^{n1} \cdot (Z_0 \cdot \exp(-E_Z/RT) + \alpha^{n2}) \quad (6)$$

Where P^m is the influence of the pressure on reaction mechanism, but it is ignored in the simulation of TSS. The superscript of m in equation (4) is the reaction order of P . $Z_0 = (A_1/A_2)$ is an autocatalytic factor, and E_Z is the difference between the activation energy of the initial stage and the autocatalytic stage. The simulation results are shown in Fig.7 and Table 4.



(a) Curve of heat release and time

(b) Curve of heat release rate dQ/dt and time

Fig.7. Simulation and experimental curves of model 1

Model 2- construction reaction model with exothermic overlapping with melting

As evidenced by the isothermal DSC and ARC results, the exothermic decomposition can occur in the solid state of TNPG. The construction of the model 2 considers the endothermic melting process and the decomposition processes in both the solid and liquid states. The reaction model is constructed as follows.

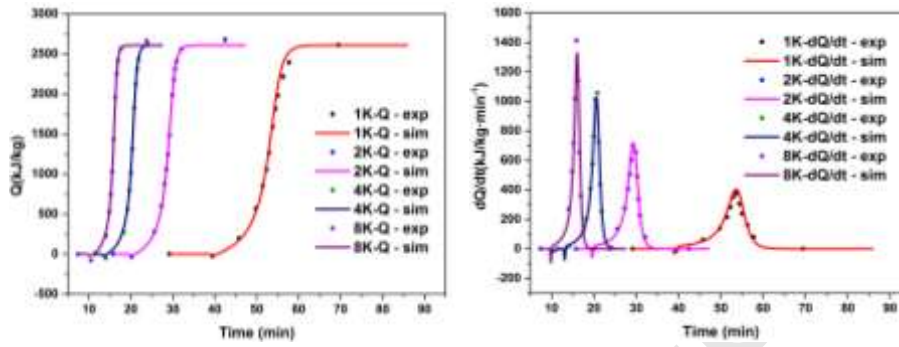


$$r_1 = A_{1,0} P^m \exp(-E/RT) (1-\alpha_1)^{n1} \cdot (Z_{0,1} \exp(-E_Z/RT) + \alpha_i^{n2}) \quad (7)$$



$$r_2 = A_2 \cdot \rho P^m \cdot \exp(-E/RT) \alpha_2^{n_1} \cdot (Z_{0,2} \exp(-E_z/RT) + \alpha_2^{n_2}) \quad (9)$$

Where $A \rightarrow B_s$ represents the autocatalytic decomposition process in the solid phase; $A \rightarrow A_{liq}$ is the melting process [28-31], according to the dynamic DSC test, the change of melting peak with temperature rise rate is not very obvious and it just a physical reaction; $A_{liq} \rightarrow B$ is the autocatalytic decomposition process in liquid phase. In equation (8), T_e is the environment temperature, T_f is the melting point of TNPG, r_f is the reaction rate of melting, and U_s is the heat transfer coefficient between TNPG and environment. The model parameters are obtained by fitting with the dynamic DSC data. The simulation results are shown in Fig. 8 and Table 4.



(a) Curve of heat release and time

(b) Curve of heat release rate of dQ/dt and time

Fig.8. Simulation and experimental curve of model 2

Comparison of the two models

Combined with the above simulation results, the relevant parameters of the constructed model are shown in Table 4. The value of Q corresponding to the decomposition process in the liquid state for model 2 is smaller than that of model 1 due to the influence of melting. Although the amount of heat of melting is small, it is not negligible. The simulation value of E for model 2 is closer to the value calculated using Friedman method. The model 2 is more in line with the decomposition of the entire process of TNPG. Model 1 only describes the decomposition process in liquid state. We cannot determine the real onset decomposition temperature for the decomposition process in the liquid state due to the thermal coupling effect that may cause large deviation with the real kinetics.

Table 4 The parameters of different reaction models

model	model 1	model 2		
	$A \rightarrow B$	$A \rightarrow B_s$	$A \rightarrow A_{liq}$	$A_{liq} \rightarrow B$
$\ln(A_0)$ (ln1/s)	$(2.57 \pm 0.36) \times 10^1$	7.85 ± 3.64	-	$(2.24 \pm 0.36) \times 10^1$
E (kJ/mol)	$(1.16 \pm 0.16) \times 10^2$	$(2.03 \pm 0.02) \times 10^2$	-	$(1.01 \pm 0.16) \times 10^2$

n	$n_1=1.18\pm 0.14$	$n_1=1.68\pm 0.14$	$n_1=1.93\pm 0.14$	$n_1=1.35\pm 0.14$
	$n_2=1.15\pm 0.14$	$n_2=1.26\pm 0.14$	$n_2=1.06\pm 0.05$	$n_2=1.70\pm 0.14$
			$n_3=1.48\pm 0.14$	
$\ln(Z_0)$	-3.88 ± 0.32	-3.88 ± 0.32	-	-0.19 ± 0.32
E_z	-1.42 ± 2.00	9.87 ± 2.00	-	8.97 ± 2.00
Q (kJ/kg)	$(2.83\pm 0.14)\times 10^3$	$(2.80\pm 0.14)\times 10^2$	$(-7.44\pm 0.14)\times 10^1$	$(2.72\pm 0.14)\times 10^3$
U_S (W/K)	-	-	$(1.26\pm 0.01)\times 10^{-4}$	-
T_f (°C)	-	-	$(1.56\pm 0.04)\times 10^2$	-

3.4.3. Verification of kinetic models

In order to verify the model 2 is suitable, the above two models are used to predict the process at different isothermal temperatures, say 161, 163 and 165 °C respectively and compare the prediction data with the experimental data. The results are shown in Fig. 9 and Table 5.

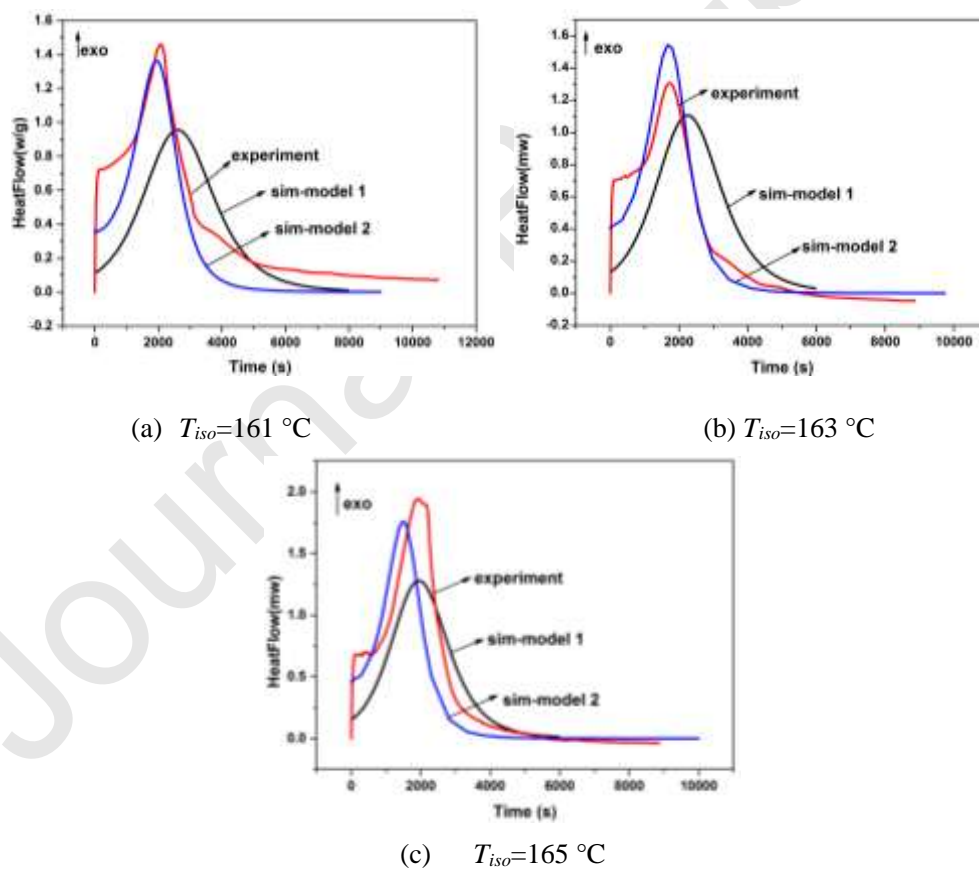


Fig. 9. Comparison between prediction and experiment data for isothermal condition
Table 5 Comparison of data between two models for predicting isothermal experiments

$T_{iso}(^{\circ}\text{C})$	Sim-Model 1		Sim-Model 2		Experiment	
	$\Delta t(\text{s})^{\text{a}}$	$\Delta H_d(\text{J/g})^{\text{b}}$	$\Delta t(\text{s})$	$\Delta H_d(\text{J/g})$	$\Delta t(\text{s})$	$\Delta H_d(\text{J/g})$
165	7889	-2800	6595	-2633	6995	-1112
163	9095	-2780	7529	-2634	7577	-1254
161	10553	-2750	8539	-2612	8899	-1718

^a Δt refer to the time from the initial decomposition to the end.

^b ΔH_d refer to the total specific heat production.

Comparing the prediction results of the two models, the values of Δt and heat release rate predicted by Model 2 is closer to the experiment data. This indicates that the decomposition processes in Fig.9 are influenced by the decomposition in the solid state and the melting process. In addition, by comparison of the heat flow profiles in Figs. 7 and 8, the model 2 can better describe the dynamic DSC data. Therefore, model 2 is more suitable for describing the thermal decomposition overlapping with melting process of TNPG.

4. Conclusions

(1) From the view of inherent safety, the solution feeding instead of traditional solid feeding reduces the risk of the entire reaction process, and the product formation was identified by related structural characterization technique.

(2) The DSC dynamic experiment indicates that TNPG is a material overlapped exothermic with endothermic, which has a high onset decomposition temperature about 174-200 °C and the average specific heat release about 3003 J/g. Moreover, it shows that the decomposition of TNPG may be autocatalytic process, and this property is further proved in the isothermal and ARC test.

(3) For the kinetic calculation of TNPG, the activation energy calculated by Friedman method and Kissinger method are similar, respectively 97-103 kJ/mol and 113 kJ/mol. The corresponding pre-exponential factor lgA is 8.8816 s^{-1} .

(4) Considering the autocatalytic decomposition model with initial stage and effects of melting on the decomposition, the TSS software is used to construct the mechanism function. It is found that the autocatalytic model 2 including the melting is closer to the actual situation of TNPG decomposition. For substances with obvious endothermic coupling with exothermic, the exothermic data should not be used to solve the reaction function. At the same time, it also provides a reference for the late kinetic prediction based on reaction model.

Acknowledgments

This work is financially supported by National Key R&D Program of China (2017YFC0804701-4)

and the Fundamental Research Funds for the Central Universities (30917011312).

References

- [1] L. Y. Zhang, J. L. Huang, Q. Ma. Study of synthesis technologic optimization and performance of 1, 3, 5-Trihydroxy - 2, 4, 6-trinitrobenzene [C]. China academic journal electronic publishing house. (2011) 181-184.
- [2] L. Y. Zhang, J. L. Huang, Q. Ma. Investigation on preparation technology and process scale-up of TNPG [C]. China academic journal electronic publishing house. (2013) 72-75.
- [3] X. M. Ma, B. D. Li, C. X. Lu, et.al. Synthesis and thermal decomposition kinetics of TATB without chloride [J]. Journal of explosive and propellants, 32(6) (2009) 24-27.
- [4] Y. Y. Wei. Preparation of 1, 3, 5-triamino-2, 4, 6-trinitrobenzene [J]. Journal of applied chemistry, (1) (1990) 70-71.
- [5] Y. Y. Wei. A new method for the preparation of DATB, TATB and their intermediates [J]. Armamentarii Acta, 13(2) (1992) 79-81.
- [6] B. T. Li, Y. M. Liang. Preparation and characterization of high-pure TATB [J]. Journal of energetic materials, (2) (1993) 6-11.
- [7] Z. Lu, J. D. Yi, Y. S. Qiu. Study of TATB on reducing chlorine content [J]. Journal of explosive and propellants, (4) (1996) 9-11.
- [8] P. R. Bowden, P. W. Leonard, J. P. Lichthard, et al. Energetic salt of trinitrophenol and melamine [C]. Biennial Aps Conference on Shock Compression of Condensed Matter. 19th Biennial APS Conference on Shock Compression of Condensed Matter, 2017.
- [9] M. Schmitt, P. Bowden, G. Avilucea et al. Investigation of energetic salts of trinitrophenol [C]//. Aps Shock Compression of Condensed Matter Meeting. APS Shock Compression of Condensed Matter Meeting Abstracts, 2017.
- [10] W. F. Liu. V. P. Sinditskii and V. Y. Egorshv. Study on the burning velocity of lead trinitrophenolate [J]. Journal of initiators and pyrotechnics, (3) (2003) 34-35.
- [11] G. Y. Zhang, L. Yang, Z. N. Zhou, et.al. Dissolution properties of trinitrophenol dissolved in deionized water [J]. Journal of energetic materials, 20(1) (2012) 83-85.
- [12] H. Y. Chen, T. L. Zhang, J. G. Zhang, et.al. The preparation, structures and thermal decomposition mechanisms of Trinitrophenolhydrate [J]. Journal of initiators and pyrotechnics, (2) (2005).
- [13] L. Y. Zhang, J. L. Huang, Q. Ma, et.al. Improvement of synthesis technology of TATB free from chloride [J]. Journal of energetic materials, 20 (5) (2012) 551-554.
- [14] L. Wang, H. Chen, T. Zhang, et al. Synthesis, characterization, thermal and explosive properties of potassium salts of trinitrophenol [J]. Journal of hazardous materials, 147(1) (2007) 576-580.

- [16] S. Vyazovkin, A. K. Burnham, M. José, Criado, et al. ICTAC kinetics committee recommendations for performing kinetic computations on thermal analysis data [J]. *Thermochimica Acta*, 520(1-2) (2011) 1-19.
- [17] H.E. Kissinger. Reaction kinetics in differential thermal analysis [J]. *Analytical Chemistry*, 29 (11) (1957) 1702-1706.
- [18] S. Chervin, G. T. Bodman. Phenomenon of autocatalysis in decomposition of energetic chemicals [J]. *Thermochimica Acta*, 392(2002) 371-383.
- [19] J. C. Oxley, J. L. Smith, E. Rogers, et al. Ammonium nitrate: thermal stability and explosively modifiers [J]. *Thermochimica Acta*, 384(1) (2002) 23-45.
- [20] B. D. Leila, F. Hans. Autocatalytic decomposition reactions, hazards and detections [J]. *Journal of hazardous materials*, 93(2002) 137-146.
- [21] R. Bertrand, H. Marco, F. Patrick, et al. Kinetic analysis of solids of the quasi-autocatalytic decomposition type: SADT determination of low-temperature polymorph of AIBN [J]. *Thermochimica Acta*, 665 (2018) 119-126.
- [22] B. Roduit, M. Hartmann, P. Folly, et al. Prediction of thermal stability of materials by modified kinetic and model selection approaches based on limited amount of experimental points [J]. *Thermochimica Acta*, 579(2014) 31-39.
- [23] H. L. Peng, L. P. Chen, G. B. Lu, et al. Thermal decomposition kinetics of Urotropin [J]. *Journal of energetic materials*, 24(5) (2016) 497-502.
- [24] T. Yang, L. P. Chen, W. H. Chen, et al. Experimental method on rapid identification of autocatalysis in decomposition reactions [J]. *Physical and Chemistry Acta*, 30(7) (2014) 1215-1222.
- [25] Y. Y. Chen, L. P. Chen, W. H. Chen, et al. Thermal decomposition characteristic and kinetics of nitro guanidine solution [J]. *Journal of energetic materials*, 25(03) (2017) 91-95.
- [26] C. X. Zhang, G. B. Lu, L. P. Chen, et al. Two decoupling methods for non-isothermal DSC results of AIBN decomposition [J]. *Journal of hazardous materials*, 285(2015) 61-68.
- [27] S. J. Shen, S. H. Wu, J. H. Chi, et al. Thermal explosion simulation and incompatible reaction of dicumyl peroxide by calorimetric technique [J]. *Journal of Thermal Analysis and Calorimetry*, 102(2) (2010) 569-577.
- [28] A. Kossoy, T. Hofelich. Methodology and software for assessing reactivity ratings of chemical systems [J]. *Process safety progress*, 22(4) (2003) 235-240.
- [29] Thermal Safety Software(TSS), ChemInform Saint Petersburg(CISP) Co., Ltd. St. Petersburg, Russia, 2017.
- [30] B. Roduit, M. Hartmann, P. Folly, et al. Parameters influencing the correct thermal safety evaluation of autocatalytic reaction [J]. *Chemical engineering transactions*, 31 (2013).

- [31] S. Y. Wang, A. Kossoy, Y. D. Yao, et al. Kinetics-based simulation approach to evaluate thermal hazards of benzaldehyde oxime by DSC tests [J]. *Thermochimica Acta*, 655(2017) 319-325.

Journal Pre-proof